

Article

Broadband Amplification in the 2.6–2.9 μm Wavelength Range in High-Purity Er^{3+} -Doped Zinc-Tellurite Fibers Pumped by Diode Lasers

Sergei Muraviev ¹, Vitaly Dorofeev ^{1,2}, Pavel Kuznechikov ³, Artem Sharafeev ^{1,2}, Maksim Koptev ¹ 
and Arkady Kim ^{1,*} 

- ¹ A.V. Gaponov-Grekhov Institute of Applied Physics of the Russian Academy of Sciences, 46 Ulyanov Str., 603950 Nizhny Novgorod, Russia; sergey.muraviev@ipfran.ru (S.M.); dorofeev@ihps-nnov.ru (V.D.); sharafeev@ihps-nnov.ru (A.S.); maksim.koptev@ipfran.ru (M.K.)
- ² G.G. Devyatykh Institute of Chemistry of High-Purity Substances of the Russian Academy of Sciences, 49 Tropinin Str., 603951 Nizhny Novgorod, Russia
- ³ Radiophysical Faculty, Nizhny Novgorod State University, 23 Gagarina Ave., 603950 Nizhny Novgorod, Russia; pavel.kuznechikov.99@mail.ru
- * Correspondence: arkady.kim@ipfran.ru

Abstract: In recent years, great progress has been made in the technology of high-purity and ultra-dry tellurite glasses, which has enabled the creation of high-purity single-mode tellurite fibers doped with rare-earth ions. This technology has made it possible to demonstrate laser generation in the range of about 2.7 μm in erbium-doped tungsten tellurite fibers. In this paper, we present an experimental study of broadband amplification in erbium-doped zinc-tellurite fibers. Zinc-tellurite glasses containing modifying components, such as Na_2O , La_2O_3 , Bi_2O_3 , or rare-earth metal oxides, are known to have noticeably lower phonon energy than heavy metal-tellurite systems, namely, tungsten tellurite glasses, which leads to better lasing output. The on-off gain of 30- and 60-cm long zinc-tellurite fibers has been measured in a wide range of diode pump powers. It has been shown for the first time that the amplification band is essentially extended, with pump power reaching over 250 nm (2600–2850 nm) at a peak power of about 40 W for a 30-cm long fiber.



Citation: Muraviev, S.; Dorofeev, V.; Kuznechikov, P.; Sharafeev, A.; Koptev, M.; Kim, A. Broadband Amplification in the 2.6–2.9 μm Wavelength Range in High-Purity Er^{3+} -Doped Zinc-Tellurite Fibers Pumped by Diode Lasers. *Photonics* **2023**, *10*, 1140. <https://doi.org/10.3390/photonics10101140>

Received: 17 August 2023
Revised: 15 September 2023
Accepted: 7 October 2023
Published: 11 October 2023



Copyright: © 2023 by the authors. Licensee MDPI, Basel, Switzerland. This article is an open access article distributed under the terms and conditions of the Creative Commons Attribution (CC BY) license (<https://creativecommons.org/licenses/by/4.0/>).

Keywords: mid-infrared fiber lasing; zinc-tellurite fibers; broadband amplification

1. Introduction

Fiber-based laser sources in the mid-infrared (mid-IR) are of great interest for a variety of applications in spectroscopy, remote sensing, and eye-safe radars in medical, chemical, and biochemical fields [1,2]. Note that there are two possible ways to create such laser sources. The first of them is to generate supercontinuum radiation in special fibers, such as chalcogenide, tellurite, or fluoride, thus providing a tunable and/or broadband mid-IR laser source [3–8]. The second way is to develop a laser source based on active fibers doped with rare-earth (RE) ions, which is, of course, preferable for obtaining more powerful laser outputs. Recently, the most significant progress has been made for laser systems based on erbium-doped specialty fibers, such as fluoride fibers, particularly with the use of ZBLAN fibers doped with erbium ions [9–12]. The $\text{Er}^{3+} {}^4\text{I}_{11/2} - {}^4\text{I}_{13/2}$ transition at 2.7–2.8 μm is currently the most convenient for laser generation because of the available high-power commercial laser diodes for the 976 nm absorption band [9]. However, despite the great success of using fluoride fibers in lasers, their commercialization is a formidable task, with difficulties stemming mainly from the drawbacks of such fibers, e.g., mechanical brittleness, tendency to crystallization, absorption of atmospheric moisture, and low softening temperature. Therefore, the development of acceptable glasses and technologies for their production and activation with RE ions to create active media is still the most important task in the development of mid-IR fiber lasers [13]. To find viable alternatives,

researchers have turned their attention from fluoride glass to multicomponent oxide glass with lower phonon energy and moderate strength [14–18]. Here, we want to emphasize the importance of continuing fiber laser developments based on tellurite glasses, which play an important role in fiber lasers, amplifiers, waveguides, and photonic crystal fibers due to their unique optical and physical properties that include lower phonon energy and better thermal ability [19]. Tellurite-based lasers operating from 1.0 to 2.1 μm with various material shapes, such as bulk glasses and fibers, were implemented in past decades, demonstrating their great potential and flexibility in the field of optoelectronic functional materials [20–23]. Last year, we demonstrated laser generation in tungstate-tellurite active fibers doped with erbium ions at $\sim 2.7 \mu\text{m}$ [24,25]. Work in this direction is continuing and is aimed at increasing the output parameters. However, in this paper, we want to draw the readers' attention to another type of tellurite fibers, namely zinc-tellurite fibers. These fibers offer important advantages which can significantly expand the range of output laser characteristics. One of the important advantages is that zinc-tellurite glasses containing some modifying components, such as Na_2O , La_2O_3 , Bi_2O_3 , or rare-earth metal oxides, have notably lower phonon energy ($\sim 750 \text{ cm}^{-1}$ for $\text{TeO}_2\text{-ZnO-La}_2\text{O}_3\text{-Na}_2\text{O}$ glass) than heavy metal-tellurite systems, like tungsten-tellurite glasses. This difference leads to a higher population of the upper laser level $^4\text{I}_{11/2}$ under continuous wave (CW) pump at the $^4\text{I}_{15/2}\text{-}^4\text{I}_{11/2}$ transition in the case of Er^{3+} -doped glass. Zinc-tellurite glasses doped with Er^{3+} are of substantial interest for erbium laser generation at $\sim 2.7 \mu\text{m}$, mostly because the upper laser level $^4\text{I}_{11/2}$ lifetime in them is twice as long as that in tungsten-tellurite glasses ($\sim 210 \mu\text{s}$ versus $\sim 110 \mu\text{s}$) [26]. It should also be noted that the transparency range of zinc-tellurite glasses is much wider and extends up to $6 \mu\text{m}$ for thin plates and planar devices and up to $4.5 \mu\text{m}$ for optical fibers. Similar to other tellurite glasses, $\text{TeO}_2\text{-ZnO}$ -based compositions with appropriate modifying additives are characterized by sufficient chemical resistance, high nonlinear optical properties, and significant solubility of rare-earth elements.

2. Materials and Methods

2.1. Zinc Tellurite Erbium-Doped Fiber

2.1.1. Glasses and Preform Preparation

The glasses of the $78\text{TeO}_2\text{-}8\text{ZnO}\text{-}1.5\text{La}_2\text{O}_3\text{-}10\text{Na}_2\text{O}\text{-}2.5\text{Er}_2\text{O}_3$ (core composition, TZLNEr, doped with $\text{Er}^{3+} 1.06 \times 10^{21} \text{ cm}^{-3}$), $76\text{TeO}_2\text{-}10\text{ZnO}\text{-}4\text{La}_2\text{O}_3\text{-}10\text{Na}_2\text{O}$ (first cladding, TZLN-1), and $66\text{TeO}_2\text{-}20\text{ZnO}\text{-}4\text{La}_2\text{O}_3\text{-}10\text{Na}_2\text{O}$ (second cladding, TZLN-2) compositions were produced by melting the oxide batch inside a sealed silica chamber at a temperature of $800 \text{ }^\circ\text{C}$ in the atmosphere of purified oxygen. The choice of the compositions of high-purity zinc-tellurite glasses is due to the high transparency in the IR region, the convenience of controlling the refractive index, the possibility of introducing relatively high concentrations of erbium, and satisfactory crystallization resistance [27].

The glasses were prepared from high-purity tellurium dioxide (TeO_2) obtained by vacuum distillation and from commercially available high-purity zinc (ZnO), lanthanum (La_2O_3), erbium (Er_2O_3) oxides, and sodium carbonate (Na_2CO_3). The total content of the 3D-transition metal impurities, most actively absorbing in the IR region, did not exceed 2 ppm wt in the initial mixture. The rare earth oxide was introduced at the stage of mixing the charge.

A monolithic double-layer preform with a core of TZLNEr glass, cladding of TZLN-1 glass, and jacketing tube of TZLN-2 glass for fiber production were fabricated by simultaneous melt extrusion. Preforms for producing tellurite fibers with a step profile of refractive index were obtained in the form of double-layered castings in which the "dry" core was protected from external impact by the cladding at all stages of optical fiber fabrication. After cutting and polishing, the preform had the following dimensions: outside diameter of 16 mm, length of 61 mm; jacketing tube: outside diameter of 16 mm, length of 56 mm. On the side surface of the preform (corresponding to the first fiber cladding), two opposite flats ($2 \times D$ shape) were made to improve the penetration of pumping modes into the core.

A number of samples of different thicknesses were cut from the preform and the tube and polished for spectroscopic studies.

2.1.2. DSC-Measurements

The NETZSCH STA-409 PC Luxx instrument was used for differential scanning calorimetry studies. Measurements were performed in an argon flow with a flow rate of 60 mL/min at a heating rate of 5 K/min. The glass samples were disc-shaped, were polished at the bottom, and had a diameter of several mm and mass of about 30–50 mg. The measurement accuracy was estimated to be ± 3 °C.

The thermograms of differential scanning calorimetry of the TZLNEr, TZLN-1, and TZLN-2 glasses are shown in Figure 1. The glass transition temperatures of all the investigated glasses were close and approximately equal to ~ 300 °C. There were no obvious thermal effects of crystallization and melting on the given curves for glasses undoped at the heating rate applied. The addition of a sufficient content of erbium oxide produced a notable impact on the resistance to crystallization for TZLNEr glasses, and there were some featureless (compared to the glass transition effect) thermal effects of crystallization and melting of crystals in the thermogram. It is known that tellurite glasses with a high erbium oxide content tend to crystallize. Therefore, the formation of samples and drawing of fibers should be carried out under the condition of minimum holding at temperatures of possible crystallization.

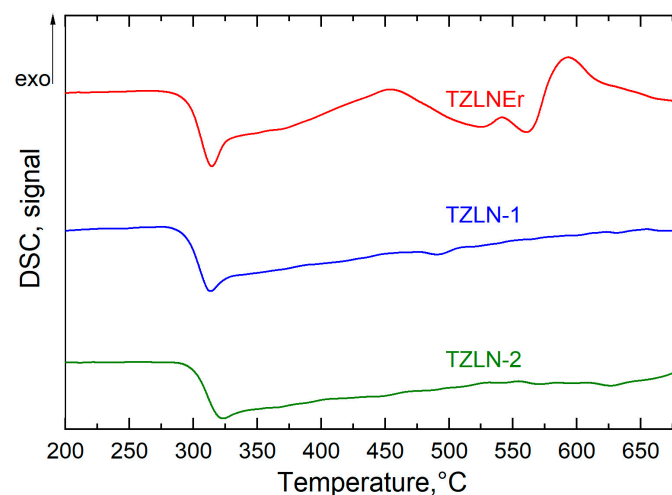


Figure 1. Thermograms of differential scanning calorimetry of TZLNEr, TZLN-1, and TZLN-2 glasses (heating rate 5 °C/min).

2.1.3. Transmission Spectra

The IR spectra were recorded by the IR Nicolet 6700 Fourier spectrometer. The absorption coefficient spectra were calculated analytically from the transmission spectra (the absorption coefficient $\alpha = -\ln(I/I_0)/L$, where L is the sample length). The visible spectra were recorded by the spectrophotometer Lambda 900. Thin discs of TZLNEr, TZLN-1 glasses with a thickness of 2.3 mm have high transmittance at a level of at least 20% in the near- and mid-IR ranges up to a wavelength of ~ 6.1 μm (Figure 2). The absence of characteristic absorption bands of 3D-transition metals and undesirable impurity RE elements throughout the transparency area confirm the low impurity content. The absorption bands of hydroxyl groups with peaks of about 2.3, 3.3, and 4.4 microns, characteristic of tellurite glasses obtained by the traditional method in open systems, were indistinguishable in the spectra of the tablets investigated. This indicates a reduced content of hydroxyl groups in the glasses. We estimated the hydroxyl group content in the core glass to be $\sim 10^{16}$ cm^{-3} , making a hole in the absorption spectrum of a 6.1 cm long preform. The content of hydroxyl groups in the TZLNEr glass was 100,000 times less than the erbium ions concentration

(10^{21} cm^{-3}). This fact guarantees the negligible impact of the hydroxyl group impurity on the luminescent properties of Er^{3+} -doped TWLBE glasses.

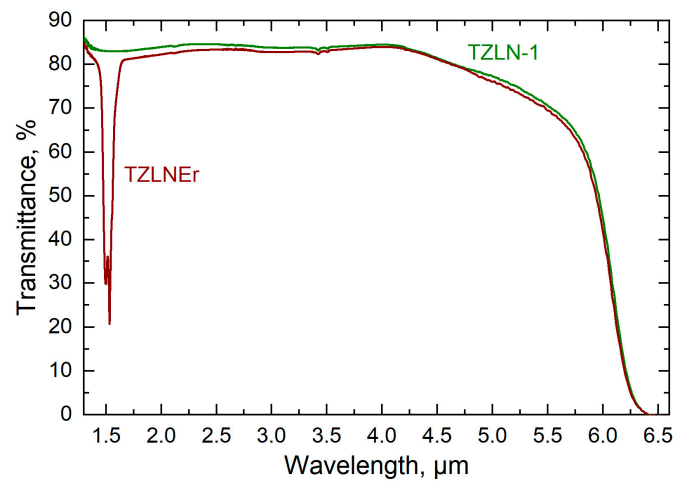


Figure 2. IR transmission spectra of TZLNEr, TZLN-1 glass samples 2.3 mm thick.

2.1.4. Optical Fiber Production and Its Optical Loss

The fibers were produced in several stages. First, the preform was stretched into a rod 4 mm in diameter; at the same stage, a fiber with a core diameter of 20 microns was drawn to measure the spectral dependence of optical loss by a Fourier spectrometer. The flats on the side surface of the stretched preform were preserved during this procedure. Next, the rod from the preform was placed into a tube, and from the obtained assembly, a single-mode fiber with a core diameter of 10 microns and two claddings was drawn (Figure 3a). In the experiments on laser amplification and generation, only a single-mode fiber was used. The numerical apertures (NA) were estimated from values of the refractive indices, which were measured using the prism-coupler Metricon-2010 at wavelengths of 969 and 1539 nm. Three scans were made during each measurement; the error was estimated to be ± 0.0003 . Table 1 contains the main characteristics of the single-mode fiber used in this work.

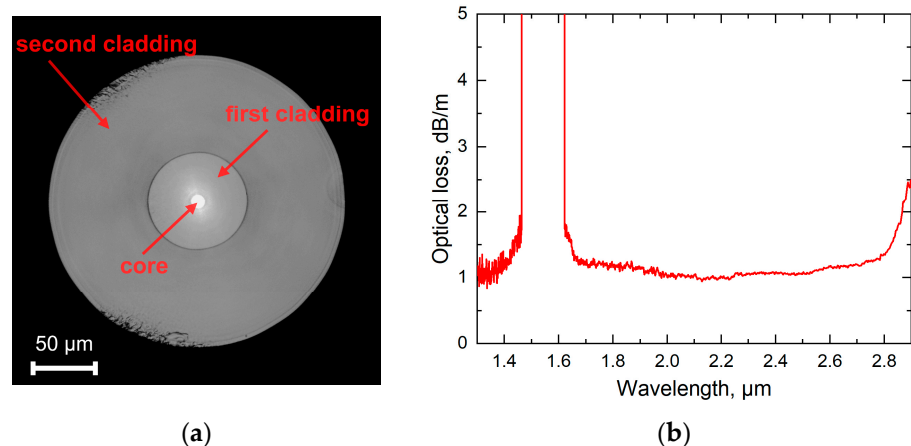


Figure 3. (a) Single-mode fiber cross-section obtained with optical microscope; (b) total optical loss of multimode fiber with core 20 μm in diameter.

Table 1. Er-doped zinc tellurite fiber parameters.

Fiber Parameter	Value
Er ₂ O ₃ concentration	2.5 mol%
Core diameter	10 μm
First cladding diameter	71 μm
Second cladding diameter	215 μm
Core NA	0.18
First cladding NA	0.42

The optical loss was measured in a multimode fiber by a cut-back method using a Bruker IFS-113v spectrometer with immersion by an indium-gallium alloy. The measurements were additionally corrected by Tm: laser cut-back measurements at a wavelength of 1.975 μm. The optical loss was of the order of 1–1.2 dB/m in the 1.75–2.75 μm range (Figure 3b). The maximal loss near 1.55 μm was due to ground state absorption at the ⁴I_{15/2} → ⁴I_{13/2} transition. The increase in losses at wavelengths over 2.75 microns was due to the absorption of hydroxyl groups and probably partly due to the effect of the multiphonon edge. The level of optical loss in the region of pumping near 980 nm did not exceed 1.3 dB/m. It can be noted that the loss in the wavelength range of about 2.75 microns, which is promising for the lasing on erbium ions, is small due to the effective removal of hydroxyl groups at the glass synthesis stage.

2.2. Experimental Setup

Since the lifetime of erbium ions at the upper laser level I_{11/2} (~210 μs) is much shorter than at the lower level I_{13/2} (~5 ms), gain and generation in such fibers are possible only in a pulsed mode with low repetition rate. The above fact also complicates the direct measurement of gain since, in this case, it is necessary to measure the low energies of the pulses following a small duty cycle, as well as the formed short seed pulses.

However, as we have shown in our previous work, the on-off gain can be measured in such fibers [26]. Such a gain does not take into account the radiation losses in the fiber and at its input and output, but it gives estimates of the cavity parameters to obtain lasing and to study the spectral dependence of the gain.

The schematic of our experimental setup for studying the amplification characteristics of an active fiber in a wide spectral range is shown in Figure 4a. An all-fiber supercontinuum generator based on a taper germanate fiber pumped by an erbium femtosecond laser was used as a seed source.

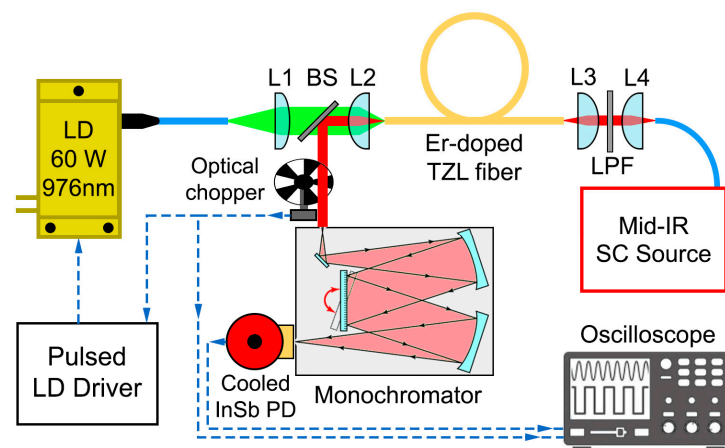


Figure 4. Experimental setup for measuring the amplifying and luminescent properties of erbium-doped zinc tellurite fibers: LD—multimode laser diode; L1—AR-coated at 976 nm plano-convex silica lens; L2–L4—uncoated plano-convex ZnSe lenses; BS—beam splitter; LPF—crystalline germanium low pass filter; PD—liquid nitrogen cooled InSb photodetector.

This source generates a supercontinuum in the 1.5–3 μm range, which completely covers the spectral amplification range of erbium TZL fibers. This source was described in detail in ref. [25]. Since the supercontinuum pulse repetition period (20 ns) is much shorter than the lifetime of erbium ions at the upper laser level (210 μs), we believe that the pulsed nature of the supercontinuum cannot affect the results of our measurements and its radiation can be considered as a quasi-continuous wave. Supercontinuum radiation was injected into the fiber under study using a pair of uncoated plano-convex zinc selenide lenses with focal lengths of 25 mm (L3, L4). Since the supercontinuum radiation in the 1.5-micron range can affect the gain in the 2.7 μm region, a low-pass filter (LPF) made of crystalline germanium and not transmitting radiation with a wavelength less than 1.8 μm was installed between the lenses. The active fiber was pumped with a low-aperture multimode fiber laser diode (LD) with a maximum output power of 60 W and a stabilized wavelength of 976 nm. Its radiation at the output of a fiber with a core/cladding diameter ratio of 105/125 μm and a numerical aperture of 0.13 was collimated by an AR-coated plano-convex lens with a focal length of 30 mm (L1). Pump radiation was launched into the fiber under study from the side opposite to the seed using an uncoated plano-convex zinc-selenium lens with a focal length of 25 mm. This setup reduces the pump spot by a factor of 1.2, providing its size of 87.5 μm at the end-face of the tellurite fiber with a slight increase in the numerical aperture. This ensures a high percentage of pump radiation input to the first cladding of the fiber under study. To extract the studied radiation, a thin plate of fused silica (BS in Figure 4) was placed between the lenses, reflecting approximately 5% of the radiation at an angle of 45 degrees. The ends of all fibers under study were cleaved at a right angle and placed for adjustment on three-coordinate optical stages (Thorlabs MBT612, Thorlabs, Newton, NJ, USA). The fibers were aligned to maximize the on-off gain since this ensures the maximum possible input of seed radiation and optimal pumping of the active fiber. To ensure spectral selectivity, the studied signal was passed through a scanning imaging monochromator (SOL Instruments MS2004i, SOL Instruments, Augsburg, Germany). A liquid nitrogen-cooled InSb photodetector (InfraRed Associates IS-0.50, Infrared Associates, Stuart, FL, USA) was used to detect radiation. Since such a detector is not capable of measuring continuous radiation, the signal under study was modulated using an optical chopper. Figure 5 shows the oscillogram of the signal from which we measured the on-off gain.

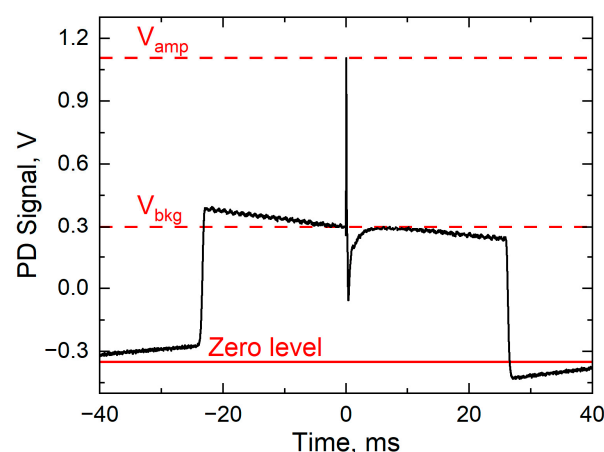


Figure 5. Oscillogram for measuring on-off gain. The pump pulse arrives at zero time. V_{bkg} —background level of unamplified signal; V_{amp} —level of amplified signal.

The seed signal passed through the fiber under study, and the monochromator and then modulated by the chopper gave the amplitude of the unamplified seed, V_{bkg} . The chopper synchronization signal was fed to a pulsed laser diode driver, which provided the generation of optical pump pulses with a duration of 210 μs and a variable amplitude. The delay of these pulses was adjusted so that the pump pulse fell approximately in the middle

of the unamplified signal pulse passed by the chopper. When the pump pulse arrived, we saw an amplified pulse on the oscillogram, followed by a dip due to absorption from the excited state. The on-off gain coefficient was calculated as the ratio of the amplitudes of the amplified pulse V_{amp} to the amplitude of the background non-amplified pulse V_{bkg} . It is worth noting that the amplitude of the amplified pulse was measured at its maximum (enlarged oscillograms of the pulses are shown in Figure 7); therefore, the measured on-off gain coefficient did not take into account the energy characteristics of the amplified pulses. To eliminate the influence of photodetector noise and ambient temperature fluctuations on the measured on-off gain, the resulting oscillograms were averaged over 128 implementations. Thus, in all the presented figures (Figures 5 and 7), already averaged oscillograms are presented. For better measurement accuracy, we set the chopper frequency to 10 Hz, so the pump pulse repetition period was 100 ms, which is sufficient for the complete unloading of the lower laser level $I_{13/2}$. This low repetition rate also allowed us to nearly double the peak pump power (compared to our previous work [25]) without the risk of thermal damage to the tellurite fiber. A slight slope of the oscillogram in Figure 5 was associated with specific features of the photodetector and amplifier operation at a low repetition rate. However, to maintain the measurement accuracy, we chose the midpoint between the minima of the signal passing through the chopper as zero.

As can be easily seen, this experimental setup can also be used to measure the luminescence spectra in erbium TZL fibers. To perform this measurement, the supercontinuum source was turned off, and the chopper was stopped in the open position. The pulsed laser diode driver operated in the internal trigger mode, as in the case of gain measurements, at a frequency of 10 Hz. The duration of the pump pulses also persisted to be 210 μs . In this case, the pulse intensity at the photodetector was proportional to the intensity of luminescence. We used a scanning monochromator to record the luminescence spectrum. To increase the sensitivity of the scheme, its entrance and exit slits were tuned to 500 μm , which nevertheless provided sufficient resolution for recording typically smooth luminescence spectra.

3. Results

3.1. Luminescent Properties of Erbium-Doped TZL Fiber

Before measuring the gain, we measured the luminescence spectra as a function of the peak pump power for an erbium TZL fiber 40 cm long. For pumping, we used pulses with a duration of 210 μs and a peak power of 10, 20, and 50 W. Figure 6 shows the measured luminescence spectra. We also measured the luminescence in the 1.5-micron range since this range falls into the telecommunication area and may also be of interest for developments in this region, especially given the fact that we use a widely available multimode laser diode pump at a wavelength of 976 nm.

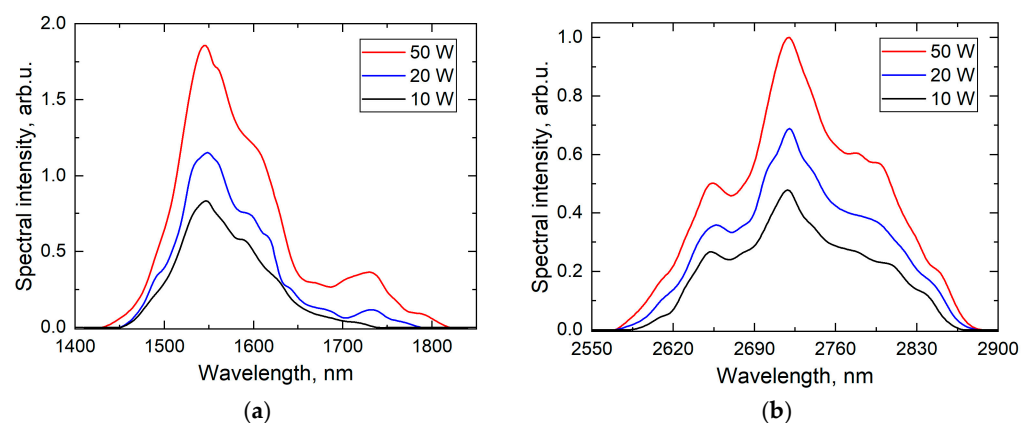


Figure 6. Experimentally measured luminescence spectra of an erbium TZL fiber 30 cm long in the 1.5-micron (a) and 2.7-micron (b) wavelength ranges depending on peak pump power. The vertical scale in panels (a,b) is the same and reflects the real ratio of luminescence powers in these ranges.

Figure 6 shows broad luminescence spectra in both the 1.5 μm and 2.7 μm ranges. The intensities of the spectra were calibrated taking into account the diffraction efficiency of the monochromator and the spectral sensitivity of the photodetector; thus they reflect the real ratio of the luminescence intensities in these ranges. Of particular interest for telecommunication applications is the long-wavelength edge of the 1.5-micron luminescence spectrum. For example, a laser on an erbium-doped tellurite fiber tunable in the 1590–1627 nm range is demonstrated in ref. [23]. Due to the property of tellurite glass to dissolve erbium ions well, such a laser provides a larger signal-to-noise ratio than lasers based on traditional silica fibers. In comparison with the work [28], where a tellurite fiber with a lower concentration of erbium (0.24 mol.%) and a weaker pumping by a single-mode laser diode with a power of 625 mW was used, an increase in luminescence radiation in the range of 1730 nm (see Figure 6a) was observed at high peak pump powers (20 W or more). This result allows us to assume the presence of gain in this region, which can make it possible to create low-noise sources based on Er:TZL fibers, both in L and U telecommunication bands or even at longer wavelengths.

However, the wavelength range of 2.7 μm is of greatest interest in this work. Luminescence was observed in the 2600–2850 nm region (see Figure 6b); the luminescence peak was at a wavelength of 2720 nm, and its position in the spectrum did not change depending on the pump power. Nevertheless, with an increase in the peak pump power, an increase in the intensity in the long-wavelength part of the luminescence spectrum relative to its short-wavelength part is observed. This increase in the luminescence intensity leads to an increase in the on-off gain in this region and makes it possible to obtain lasing in the 2.8 μm region with an increase in the laser diode pump power. We also measured the ratio of the maximum values of the luminescence intensity at wavelengths of 1550 nm and 2720 nm, which was 1.72 for a pump power of 10 W, 1.67 for 20 W, and 1.82 for 50 W, respectively. Comparison with the work [28], where the spectral intensity of the luminescence in the 1.5 μm region exceeded that for the 2.7 μm region by a factor of 5, allows us to speak about better properties of our fiber in terms of amplification and lasing in the mid-IR.

3.2. On-off Gain Performance of Erbium-Doped TZL Fiber

According to the luminescence spectra measurements, we studied the on-off gain in the 2550–2900 nm wavelength range. The wavelength at which the maximum on-off gain was observed for all diode pump powers available to us was 2710 \pm 10 nm. Before proceeding directly to measuring the gain spectra, we studied the shape of the amplified pulses at the photodetector output using a digital oscilloscope, while the wavelength at the monochromator was set to 2710 nm. Figure 7 shows oscillograms of amplified pulses at different peak pump powers: 10, 20, 30, and 40 W, which correspond to pump pulse energies of 2.1, 4.2, 8.4, and 16.8 mJ, respectively. It is worth noting that the pulses in Figure 7 represent the central part of the oscillogram shown in Figure 5, enlarged along the time axis. A piece of erbium TZL fiber 40 cm long was used in these measurements. One can see that the amplified pulses at all pump powers have a structure with one pronounced peak. At low pump levels, the amplified pulses had a fairly flat and broad peak, while with increasing pump power, the peak became sharper, and its position in time was closer to the leading edge of the pump pulse. At high pump powers, we also observed a dip in the seed signal immediately after turning off the pump associated with strong absorption from the excited state caused by the long lifetime of the lower laser level.

Compared to our previous work [25], we did not observe any multipulse dynamics of amplified pulses despite the fact that significantly higher pump levels were used. We believe that the reason for this result is the twice-longer lifetime of the upper laser level in TZL fibers compared to TWL fibers, leading to the damping of possible oscillations.

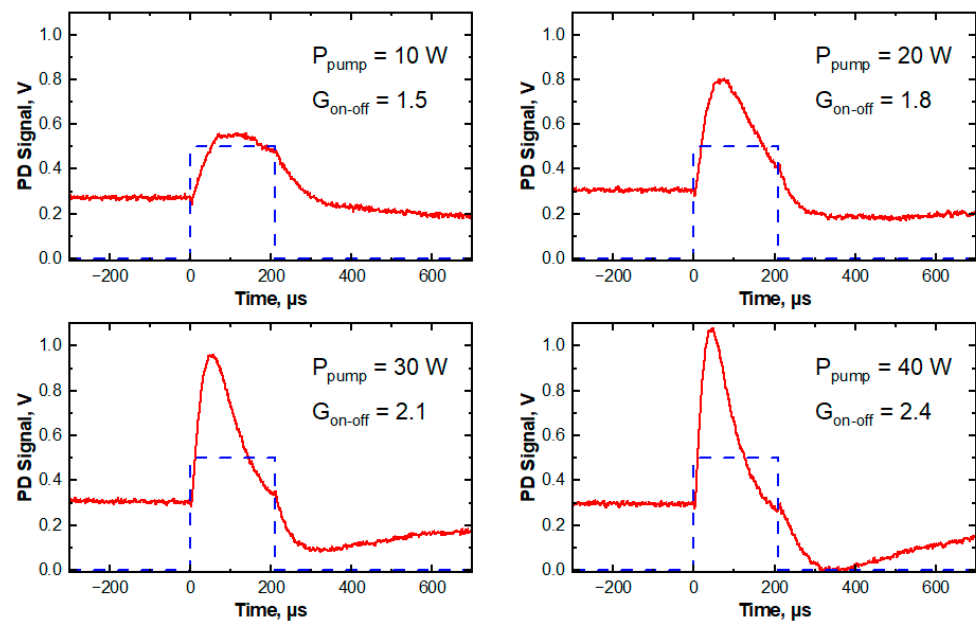


Figure 7. The shape of the pulses amplified in a 40-cm piece of Er:TZL fiber (red line). A trace indicating the duration of the pump pulse (dashed blue line).

To study the on-off amplification, we used two segments of tellurite fiber 30 and 60 cm long; in view of the high concentration of erbium ions, the study of longer segments seemed inappropriate. We estimated the on-off gain by the ratio of the amplitude of the amplified pulse at its peak to the unamplified radiation. This approach neglects the shape of the amplified pulses and, accordingly, their energy. However, as shown earlier, lasing pulses in erbium-doped tellurite fibers usually have a duration of several microseconds [24], which is much less than the width of the amplified pulses. Therefore, we believe that this approach is fully applicable to assess the possibility of lasing in such fibers. The spectral dependence of the on-off gain in erbium TZL fibers as a function of the peak pump power is shown in Figure 8.

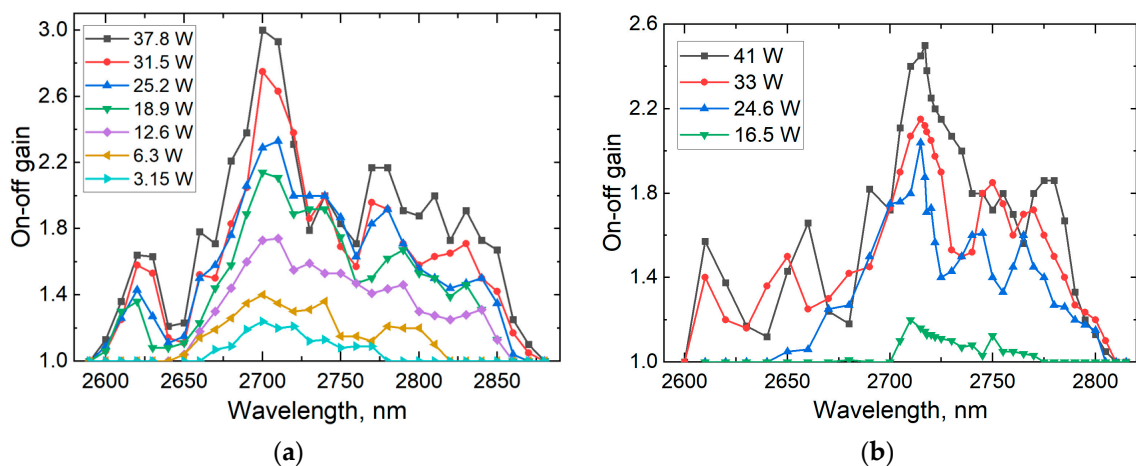


Figure 8. Spectral dependence of on-off gain as a function of peak pump power for Er:TZL fibers 30 cm (a) and 60 cm (b) long.

Due to the manual measurement process, the gain spectra have a discrete structure, with intermediate values being approximated by straight lines. As can be seen from Figure 8, amplification begins already at peak pump powers of 3 W. The wavelength of maximum gain, regardless of the length of the fiber under study and the pump power, is in the range of $2710 \pm 10 \text{ nm}$. However, the maximum gain was obtained on a 30-cm

long fiber segment, which, in our opinion, is due to its better pumping and lower losses for seed radiation. For all lengths of the fibers under study, a significant broadening of the gain spectra was observed with increasing pump power. Thus, for a fiber length of 30 cm at a peak pump power of 6.3 W, the gain spectrum width is 180 nm, while at a maximum pump power of 37.8 W, it is 290 nm. For a fiber length of 60 cm, the spectral width also increases from 75 nm for a pump power of 16.5 W to 210 nm for a pump power of 41 W. The gain spectra for a fiber length of 30 cm are quite smooth, without strongly pronounced dips and peaks (with the exception of a peak at a wavelength of 2710), which indicates the possibility of constructing sources of ultrashort pulses based on such fibers or sources tunable over a wide wavelength range.

For a better understanding of the dependence of the gain on the fiber length, we also show in Figure 9 its dependence on the pump power for two fiber lengths measured at the wavelength of maximum gain—2710 nm.

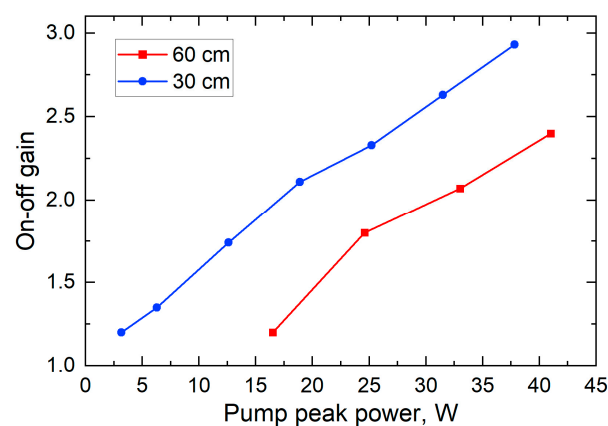


Figure 9. On-off gain versus peak pump power for 30-cm (blue line) and 60-cm (red line) long Er:TZL fibers.

The slope of the gain versus peak pump power curves for the 30- and 60-cm segments is practically the same and amounts to 0.05 W^{-1} . However, for the optimal length of 30 cm, a significantly lower gain threshold (3.15 W vs. 16.5 W) and the highest value of the maximum gain (2.93 vs. 2.4) were observed. Thus, the fiber studied in this work makes it possible to achieve an on-off gain of about three per pass, which, according to our calculations (including losses), is sufficient to ensure stable lasing in the pulsed mode. Also, during all the experiments, which usually lasted several hours, we did not notice any degradation of the fiber under study caused by pumping or exposure to atmospheric moisture.

4. Discussion

Coherent fiber sources in the wavelength range of about $2.7 \mu\text{m}$ have long attracted the attention of researchers, primarily due to the large number of applications of such lasers, ranging from precision gas spectroscopy to biomedical ones. Among such sources, lasers based on erbium-doped fibers ($I_{11/2} \rightarrow I_{13/2}$ transition) are especially noted since they can use widely available and low-cost laser diodes at a wavelength of 976 nm as pumping. At present, only lasers based on fluorine-zirconate fibers (ZBLAN) are capable of efficient generation and amplification at a wavelength of $2.7 \mu\text{m}$. However, the physicochemical properties of such fibers, e.g., low strength and a tendency to crystallize and absorb atmospheric moisture, do not allow lasers based on them to occupy their niche among commercial mid-IR sources. One promising medium is multicomponent oxide glasses based on tellurium oxide (tellurite glasses). Such glasses are distinguished by high chemical stability, resistance to crystallization, low level of optical losses in the wavelength range of $2.7 \mu\text{m}$, and good solubility of erbium ions. At the same time, their physical properties

make it easy to draw high-quality optical fibers from them, simply obtaining the required difference in refractive indices due to a slight change in the composition of the glass.

Recently, we studied erbium-doped tellurite fibers based on glass with $\text{TeO}_2\text{-WO}_3\text{-La}_2\text{O}_3\text{-Bi}_2\text{O}_3$ composition (TWL). The triple-clad design of such fibers consisted of a core 7.5 μm in diameter doped with 0.4 mol. % erbium ions and three claddings with diameters of 23, 66, and 211 μm , respectively. The large difference in the lifetimes of the upper and lower laser levels in such a fiber (110 μs versus 7 ms) made it impossible to amplify and lase in the continuous-wave mode. However, we showed that in the pulsed mode, such fibers can provide a high (about five) on-off gain per pass [25]. We also succeeded for the first time in achieving laser generation at a wavelength of 2.7 μm in such a fiber [24]. However, the generation parameters were far from those achieved in ZBLAN fibers; we obtained only sub-microjoule pulses with a duration of several microseconds. Thus, erbium tellurite fibers still have a long way to go in terms of optimization and improvement.

This paper is a continuation of this work. Here, we have used a tellurite fiber based on glass of a different composition— $\text{TeO}_2\text{-ZnO-Al}_2\text{O}_3\text{-Na}_2\text{O-Fe}_2\text{O}_3$ (TZL). This composition has made it possible to double the lifetime of the upper laser level (up to 210 μs), and the high concentration of erbium ions in the core (2.5 mol.%) has ensured a shorter lifetime of the lower laser level (5 ms). With regard to pulsed generation in such fibers, a longer lifetime of the upper laser level contributes to a greater accumulation of energy and, accordingly, a higher energy of the generated pulses. The shorter lifetime of the lower laser level makes it possible, in turn, to increase the pulse repetition rate (because less time is required to unload the lower level), which allows for increasing the average output power of the laser. The physicochemical properties of such fibers are similar to those of tungstate tellurite (TWL) and, accordingly, inherit all the advantages of TWL. We have also optimized the physical design of the fiber by creating a simple double-clad structure with a core diameter of 10 μm and the first and second cladding diameters of 71 and 215 μm , respectively. This design makes it possible to most efficiently launch multimode pump radiation into the first cladding, propagating through a standard fiber with a core/cladding diameter ratio of 105/125 μm while at the same time providing high pump brightness necessary for good absorption in the erbium-doped core. We have studied in detail the luminescent and amplifying properties of TZL fibers, including their temporal characteristics and spectral dependences. We have shown broad (over 250 nm) on-off gain spectra, indicating the possibility of creating ultrashort-pulsed or widely tunable sources based on such fibers. Our next step will be to investigate lasing in this TZL fiber, and we believe that the improved performance compared to our previous TWL fiber will enable a more efficient and powerful laser.

5. Conclusions

This article is a continuation of our previous works on the study of erbium-doped tellurite fibers for generation in the 2.7 μm region. Here, we have presented a novel zinc tellurite fiber that features a longer upper laser lifetime, a higher erbium ion concentration, and an improved design optimized for pumping by widely used 976 nm fiber laser diodes with a 105/125 fiber core/cladding diameter ratio. We have studied in detail the luminescent and amplifying properties of this fiber at pumping levels twice as high as our previous studies. We have presented the spectral dependences of the on-off gain at various pump powers and active fiber lengths. It has been shown that the amplification band can be essentially extended over 250 nm (from 2600 to 2850 nm) with pump power, and the maximum gain can reach a value of 3, allowing erbium-doped zinc-tellurite fibers to be considered as an effective active element in creating laser systems of practical use.

Author Contributions: Conceptualization, V.D. and A.K.; methodology, S.M.; software, P.K.; validation, V.D., S.M. and M.K.; formal analysis, M.K.; investigation, S.M. and M.K.; resources, S.M., V.D. and A.S.; data curation, M.K. and A.K.; writing—original draft preparation, S.M.; writing—review and editing, M.K., V.D. and A.K.; visualization, S.M. and M.K.; supervision, A.K.; project administra-

tion, A.K.; funding acquisition, A.K. All authors have read and agreed to the published version of the manuscript.

Funding: This research was supported by the Center of Excellence, «Center of Photonics», funded by the Ministry of Science and Higher Education of the Russian Federation, contract No. 075-15-2022-316.

Institutional Review Board Statement: Not applicable.

Informed Consent Statement: Not applicable.

Data Availability Statement: Data underlying the results presented in this paper are not publicly available at this time but may be obtained from the authors upon reasonable request.

Conflicts of Interest: The authors declare no conflict of interest.

References

- Ebrahim-Zadeh, M.; Sorokina, I.T. (Eds.) *Mid-Infrared Coherent Sources and Applications*; NATO Science for Peace and Security Series B: Physics and Biophysics; Springer: Dordrecht, The Netherlands, 2008; ISBN 978-1-4020-6439-5.
- Jackson, S.D. Towards High-Power Mid-Infrared Emission from a Fibre Laser. *Nat. Photonics* **2012**, *6*, 423–431. [[CrossRef](#)]
- Petersen, C.R.; Møller, U.; Kubat, I.; Zhou, B.; Dupont, S.; Ramsay, J.; Benson, T.; Sujecki, S.; Abdel-Moneim, N.; Tang, Z.; et al. Mid-Infrared Supercontinuum Covering the 1.4–13.3 μm Molecular Fingerprint Region Using Ultra-High NA Chalcogenide Step-Index Fibre. *Nat. Photonics* **2014**, *8*, 830–834. [[CrossRef](#)]
- Robichaud, L.-R.; Fortin, V.; Gauthier, J.-C.; Châtigny, S.; Couillard, J.-F.; Delarosbil, J.-L.; Vallée, R.; Bernier, M. Compact 3–8 μm Supercontinuum Generation in a Low-Loss As_2Se_3 Step-Index Fiber. *Opt. Lett.* **2016**, *41*, 4605. [[CrossRef](#)] [[PubMed](#)]
- Kedenburg, S.; Strutynski, C.; Kibler, B.; Froidevaux, P.; Désévéday, F.; Gadret, G.; Jules, J.-C.; Steinle, T.; Mörz, F.; Steinmann, A.; et al. High Repetition Rate Mid-Infrared Supercontinuum Generation from 13 to 53 μm in Robust Step-Index Tellurite Fibers. *J. Opt. Soc. Am. B* **2017**, *34*, 601. [[CrossRef](#)]
- Yin, K.; Zhang, B.; Yao, J.; Yang, L.; Liu, G.; Hou, J. 19–36 μm Supercontinuum Generation in a Very Short Highly Nonlinear Germania Fiber with a High Mid-Infrared Power Ratio. *Opt. Lett.* **2016**, *41*, 5067. [[CrossRef](#)]
- Yang, L.; Zhang, B.; Jin, D.; Wu, T.; He, X.; Zhao, Y.; Hou, J. All-Fiberized, Multi-Watt 2–5- μm Supercontinuum Laser Source Based on Fluoroindate Fiber with Record Conversion Efficiency. *Opt. Lett.* **2018**, *43*, 5206. [[CrossRef](#)]
- Yang, L.; Zhang, B.; He, X.; Deng, K.; Liu, S.; Hou, J. High-Power Mid-Infrared Supercontinuum Generation in a Fluoroindate Fiber with over 2 W Power beyond 3.8 μm . *Opt. Express* **2020**, *28*, 14973. [[CrossRef](#)] [[PubMed](#)]
- Aydin, Y.O.; Fortin, V.; Maes, F.; Jobin, F.; Jackson, S.D.; Vallée, R.; Bernier, M. Diode-Pumped Mid-Infrared Fiber Laser with 50% Slope Efficiency. *Optica* **2017**, *4*, 235. [[CrossRef](#)]
- Aydin, Y.O.; Fortin, V.; Vallée, R.; Bernier, M. Towards Power Scaling of 28 μm Fiber Lasers. *Opt. Lett.* **2018**, *43*, 4542. [[CrossRef](#)]
- Shen, Y.; Wang, Y.; Zhu, F.; Ma, L.; Zhao, L.; Chen, Z.; Wang, H.; Huang, C.; Huang, K.; Feng, G. 200 MJ, 13 Ns Er:ZBLAN Mid-Infrared Fiber Laser Actively Q-Switched by an Electro-Optic Modulator. *Opt. Lett.* **2021**, *46*, 1141. [[CrossRef](#)]
- Luo, H.; Yang, J.; Li, J.; Liu, Y. Tunable Sub-300 Fs Soliton and Switchable Dual-Wavelength Pulse Generation from a Mode-Locked Fiber Oscillator around 2.8 Mm. *Opt. Lett.* **2021**, *46*, 841. [[CrossRef](#)] [[PubMed](#)]
- Jackson, S.D.; Jain, R.K. Fiber-Based Sources of Coherent MIR Radiation: Key Advances and Future Prospects (Invited). *Opt. Express* **2020**, *28*, 30964. [[CrossRef](#)] [[PubMed](#)]
- Guo, Y.; Li, M.; Hu, L.; Zhang, J. Intense 27 μm Emission and Structural Origin in Er^{3+} -Doped Bismuthate (Bi_2O_3 - GeO_2 - Ga_2O_3 - Na_2O) Glass. *Opt. Lett.* **2012**, *37*, 268. [[CrossRef](#)] [[PubMed](#)]
- Ma, Y.; Guo, Y.; Huang, F.; Hu, L.; Zhang, J. Spectroscopic Properties in Er^{3+} Doped Zinc- and Tungsten-Modified Tellurite Glasses for 2.7 μm Laser Materials. *J. Lumin.* **2014**, *147*, 372–377. [[CrossRef](#)]
- Chen, F.; Wei, T.; Jing, X.; Tian, Y.; Zhang, J.; Xu, S. Investigation of Mid-Infrared Emission Characteristics and Energy Transfer Dynamics in Er^{3+} Doped Oxyfluoride Tellurite Glass. *Sci. Rep.* **2015**, *5*, 10676. [[CrossRef](#)]
- Yu, J.; Zhang, M.; Lu, X.; Du, Y.; Brambilla, G.; Jia, S.; Wang, S.; Wang, P. Broadband 2.7 μm Mid-Infrared Emissions in Er^{3+} -Doped PbO - PbF_2 - Bi_2O_3 - Ga_2O_3 Glasses. *Opt. Lett.* **2020**, *45*, 4638. [[CrossRef](#)]
- Zhang, Y.; Xia, L.; Li, C.; Ding, J.; Li, J.; Zhou, Y. $\text{Dy}^{3+}/\text{Er}^{3+}/\text{Tm}^{3+}$ Tri-Doped Tellurite Glass with Enhanced Broadband Mid-Infrared Emission. *Opt. Laser Technol.* **2022**, *149*, 107904. [[CrossRef](#)]
- Rivera, V.A.G.; Manzani, D. (Eds.) *Technological Advances in Tellurite Glasses: Properties, Processing, and Applications*; Springer Series in Materials Science; Springer International Publishing: Cham, Switzerland, 2017; Volume 254, ISBN 978-3-319-53036-9.
- Ohishi, Y.; Mori, A.; Yamada, M.; Ono, H.; Nishida, Y.; Oikawa, K. Gain Characteristics of Tellurite-Based Erbium-Doped Fiber Amplifiers for 15- μm Broadband Amplification. *Opt. Lett.* **1998**, *23*, 274. [[CrossRef](#)]
- Libatique, N.J.C.; Tafoya, J.; Viswanathan, N.K.; Jain, R.K.; Cable, A. 'Field-Usable' Diode-Pumped ~120 Nm Wavelength-Tunable CW Mid-IR Fibre Laser. *Electron. Lett.* **2000**, *36*, 791. [[CrossRef](#)]
- Dong, J.; Wei, Y.Q.; Wonfor, A.; Pentyl, R.V.; White, I.H.; Lousteau, J.; Jose, G.; Jha, A. Dual-Pumped Tellurite Fiber Amplifier and Tunable Laser Using $\text{Er}^{3+}\text{Ce}^{3+}$ Codoping Scheme. *IEEE Photonics Technol. Lett.* **2011**, *23*, 736–738. [[CrossRef](#)]

23. Fu, S.; Zhu, X.; Wang, J.; Wu, J.; Tong, M.; Zong, J.; Li, M.; Wiersma, K.; Chavez-Pirson, A.; Peyghambarian, N. L-Band Wavelength-Tunable Er³⁺-Doped Tellurite Fiber Lasers. *J. Lightwave Technol.* **2020**, *38*, 1435–1438. [[CrossRef](#)]
24. Muraviev, S.V.; Dorofeev, V.V.; Motorin, S.E.; Koltashev, V.V.; Koptev, M.Y.; Kim, A.V. Lasing at 2.72 μm in an Er³⁺-Doped High-Purity Tungsten–Tellurite Glass Fiber Laser. *Opt. Lett.* **2022**, *47*, 5821. [[CrossRef](#)] [[PubMed](#)]
25. Muraviev, S.V.; Dorofeev, V.V.; Motorin, S.E.; Koptev, M.Y.; Kim, A.V. Broadband Gain Performance in the Mid-IR Using Supercontinuum: 2.7 μm Gain in High-Purity Er³⁺ Doped Tungsten Tellurite Glass Fibers. *Appl. Opt.* **2022**, *61*, 9701. [[CrossRef](#)] [[PubMed](#)]
26. Gomes, L.; Oermann, M.; Ebendorff-Heidepriem, H.; Ottaway, D.; Monroe, T.; Felipe Henriques Librantz, A.; Jackson, S.D. Energy Level Decay and Excited State Absorption Processes in Erbium-Doped Tellurite Glass. *J. Appl. Phys.* **2011**, *110*, 083111. [[CrossRef](#)]
27. Kut'in, A.M.; Plekhovich, A.D.; Balueva, K.V.; Motorin, S.E.; Dorofeev, V.V. Thermal Properties of High Purity Zinc-Tellurite Glasses for Fiber-Optics. *Thermochim. Acta* **2019**, *673*, 192–197. [[CrossRef](#)]
28. Anashkina, E.A.; Andrianov, A.V.; Dorofeev, V.V.; Kim, A.V.; Koltashev, V.V.; Leuchs, G.; Motorin, S.E.; Muravyev, S.V.; Plekhovich, A.D. Development of Infrared Fiber Lasers at 1555 Nm and at 2800 Nm Based on Er-Doped Zinc-Tellurite Glass Fiber. *J. Non-Cryst. Solids* **2019**, *525*, 119667. [[CrossRef](#)]

Disclaimer/Publisher's Note: The statements, opinions and data contained in all publications are solely those of the individual author(s) and contributor(s) and not of MDPI and/or the editor(s). MDPI and/or the editor(s) disclaim responsibility for any injury to people or property resulting from any ideas, methods, instructions or products referred to in the content.